Transactions of the Materials Research Society of Japan 29[6] 2849-2852 (2004)

Magnetic Field Effect for Thermoelectric Conversion : A Proposal for Nernst-Seebeck Element

Shin Yamamoto, Makoto Hamabe, Hideaki Takahashi, Satarou Yamaguchi, Haruhiko Okumura*, Ichiro Yonenaga**, Takako Sasaki**, and Kazuo Watanabe**

Department of Electric Engineering, Chubu University, 1200 Matsumoto-chou, Kasugai, Aichi, 487-8501, Japan
Fax: 81-568-51-9725, e-mail: e99174@isc.chubu.ac.jp
* Matsusaka University, Matsusaka, Mie, 515-8511, Japan
** Institute for Material Research, Tohoku University, 2-1-1 Katayama Aoba-ku, Sendai, Miyagi, 980-8577, Japan

We have studied the magnetic field effects of the thermoelectric properties aiming to improve the thermoelectric energy conversion efficiency. In the magnetic field, the sum of the Nernst voltage and the Seebeck voltage arises between the diagonal corners on the rectangular material since the direction of the Nernst electric field is perpendicular to that of the Seebeck electric field. This corresponds to the increment of the effective thermoelectric power. We named the thermoelectric element using this diagonal voltage as "the Nernst-Seebeck element". We measured the transport coefficients of the polycrystalline bismuth in the magnetic field from 100 K to 290 K to estimate the performance of the Nernst-Seebeck element. The measured quasi-figure-of-merit of the bismuth Nernst-Seebeck element increased, compared with those in the zero magnetic field, in spite of the remarkable increase of the magnetoresistance. The quasi-figure-of-merit z_{N+S} of a square bismuth increased by 3.7 times at 150 K. We considered the geometry effect of the Nernst-Seebeck element and found the remarkable improvement by using geometric effect
Key words: polycrystalline bismuth, Seebeck effect, Nernst effect, magnetic field effect

1. INTRODUCTION

Bismuth (Bi) and its alloys have high potentials as the thermoelectric materials, in particular, at temperatures lower than the room temperature and they are often employed for the thermoelectric energy conversion in the use of the cold heat[1]. Use of the magnetic field effect is one of the methods to improve the thermoelectric performance of the Bi and its alloys. Wolfe and Smith reported that the thermoelectric figure-of-merit of an undoped *n-type* bismuth-antimony (Bi-Sb) alloy enhances in the transverse magnetic field at 100 K [2]. Yim and Amith also showed the magnetic field improves the thermoelectric figure-of-merit for undoped *n-type* Bi-Sb alloys and for a Sn-doped *p-type* Bi-Sb alloy [3].

For the polycrystalline Bi, Brochin et al. measured the electric resistivity, the Seebeck coefficient and the thermal conductivity in the zero magnetic field, and showed that the polycrystalline Bi also has a high figure of merit [4]. Since the Seebeck coefficient of a single crystal Bi also increases with applying transverse magnetic field [5][6], the polycrystalline Bi also has a potential to improve the figure of merit by the magnetic field effect. On the other hand, the single crystal Bi has a high Nernst effect when the magnetic field is applied parallel to the binary axis at low temperature [5][6][7]. De Sande *et al.* showed the Nernst coefficient of the polycrystalline Bi is also high at the room temperature [8].

We have proposed to use the sum of the Nernst voltage and the Seebeck voltage (the Nernst+Seebeck effect) in the magnetic field, to increase the effective thermoelectric power [9][10]. We named the thermo-electric element, which uses the Nernst+Seebeck effect, as "the Nernst-Seebeck element".

In this work, we measured the magnetic field effect of the transport coefficients for the polycrystalline Bi from 100 K to 290 K and confirmed the improvement of the thermoelectric performance as the Nernst-Seebeck element. The geometric effect was also measured to prove the remarkable improvement of the Nernst-Seebeck element.

2. PRINCIPLE OF NERNST-SEEBECK ELEMENT

Figure 1 illustrates the principle of the Nernst-Seebeck element. Standard thermoelectric elements presuppose to use only the Seebeck effect. The Seebeck electric field is in the direction of the temperature gradient. On the other hand, the Nernst electric field is perpendicular to both the magnetic field and the temperature gradient. Hence, the potential difference V_{AB} between the diagonal two electrodes A and B is the sum of the Nernst voltage V_N and the Seebeck voltage V_S. The effective thermoelectric power of this Nernst -Seebeck element $\alpha_{N+S} = V_{12}/\Delta T = (V_N+V_S)/\Delta T$ becomes larger than that of the Seebeck element, where ΔT is the

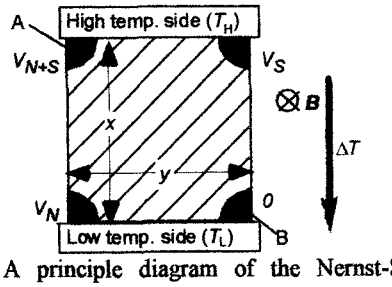

Fig. 1 A principle diagram of the Nernst-Seebeck element.

temperature difference.

The following four magnetic field effects relate to the thermoelectric performance of the Nernst-Seebeck element;

1) the variation of the Seebeck coefficient α_S,
2) the increment of the electric resistivity η,
3) the reduction of the thermal conductivity κ, and
4) the arising of the Nernst effect *NB*.

Considering the thermoelectric figure-of-merit for the Seebeck element, $Z_S = \alpha_S^2 / \eta\kappa$ [11], increasing α_S and decreasing κ enhance Z_S, while increasing η reduces Z_S. On the other hand, the Nernst effect arises in the magnetic field. The expression of the thermoelectric figure-of-merit of the Nernst element is $Z_N = (NB)^2 / \eta\kappa$; where N is the Nernst coefficient and B is the applied magnetic field [12]. For the Nernst-Seebeck element, the internal electric resistance in the element R considerably depend on the geometry of the thermoelectric material and those of the electrodes A and B in Fig. 1; therefore, we used to estimate the following quasi-figure-of-merit z_{N+S} instead of the figure-of-merit;

$$z_{N+S} = \frac{\alpha_{N+S}^2}{R\kappa} \quad (1)$$

Since the Nernst voltage V_N has the geometry dependence as $V_N = (y/x)NB\Delta T$, where x is the length and y is the width of the thermoelectric material, z_{N+S} also has the geometry dependence as follows;

$$z_{N+S} = \frac{(V_N + V_S)^2 / \Delta T^2}{R\kappa} = \frac{\{(y/x)NB + \alpha_S\}^2}{R\kappa} \quad (2)$$

3. SETUP

Figure 2 illustrates a schematic diagram of the sample to measure the transport properties of the polycrystalline Bi (99.999%, Furuuchi Chemical Corp.). The geometry of the sample is 10 mm in length, 10 mm in width, and 2 mm in thickness. A copper block is attached to the one side of the sample as the heat sink. A cryocooler connected to the heat sink controls the base temperature of the sample from 100 K to 290 K. Another copper block with a foil heater is attached on the opposite side of the sample as the heat source to produce ΔT up to about 10 K. Two spring coils connect the heat-source copper block to the heat-sink copper block to keep good thermal contacts between the sample and the heat sink and source blocks. A insulating sheet is inserted between the sample and each copper block to avoid the Nernst voltage shortcircuited on the copper block. The essential properties for the insulating sheet are the high electric resistance and the high thermal conductivity. We successfully achieve this properties with using a very thin paper coated by the thermal-conductive grease.

The sample is installed in the vacuum vessel with pressure less than 0.01 Pa. A superconducting magnet system generated a magnetic field up to ±1.5 T perpendicular to the sample, as shown in Fig. 1.

The Seebeck voltage V_S, the Nernst voltage V_N, and the Nernst+Seebeck voltage V_{N+S} are simultaneously measured by using the electrodes placed on the four corners of the rectangle sample. Temperatures of the both sides of the sample T_H and T_L are measured using

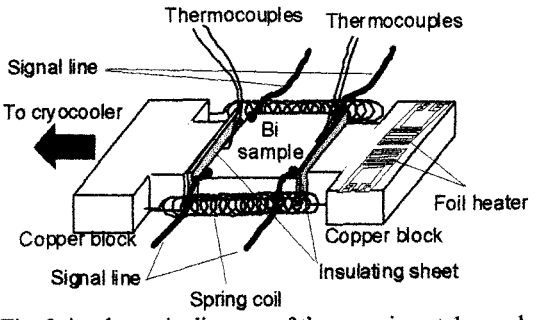

Fig. 2 A schematic diagram of the experimental sample.

copper-constantan thermocouples fixed on the sample edge. Temperature difference ΔT is equal to $T_H - T_L$. Thermoelectric powers α_S, α_N, and α_{S+N} were carefully estimated from the variation of the potential difference for the two different ΔT: when the heater is on or off. The steady-state method is employed to measure κ, where κ was conveniently estimated from the input power to the heater and the variation of ΔT. The electric resistance (the diagonal resistance) R was measured between the diagonally-placed two electrodes with the four-probe method

4. RESULTS

4.1 Transport coefficients of the polycrystalline Bi

Figure 3 shows the thermoelectric power of the Seebeck effect (the Seebeck coefficient) α_S vs the magnetic field B. The magneto-Seebeck effect increases the absolute value of α_S at all temperatures. The temperature dependence of the magnetic field effect for α_S is similar from 200 K to 290 K and remarkably increases at 100 K.

Figure 4 shows the magnetic field dependences of the thermoelectric power of the Nernst effect α_N (=*NB*). Although the polarity of α_N reverses in the low magnetic field near 0 T in the single crystal [6][7], it does not reverse in the polycrystal. Figure 5 shows the temperature dependence of the Nernst coefficient N measured at B = 1.5 T. The Nernst coefficient for the single crystal Bi by Michenaud *et al.* [6] and Sugihara [7] and that for the polycrystalline Bi at the room temperature by de Sande *et al.* [8] are also shown in Fig. 5 for the comparison. In Fig. 5, *N*231 corresponds to the single crystal Nernst coefficient when the heat flow is in

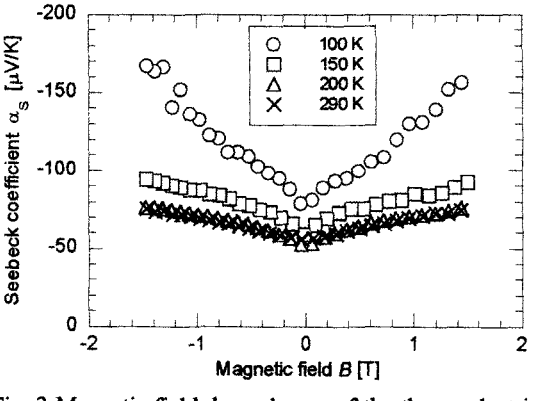

Fig. 3 Magnetic field dependences of the thermoelectric power of the Seebeck effect α_S.

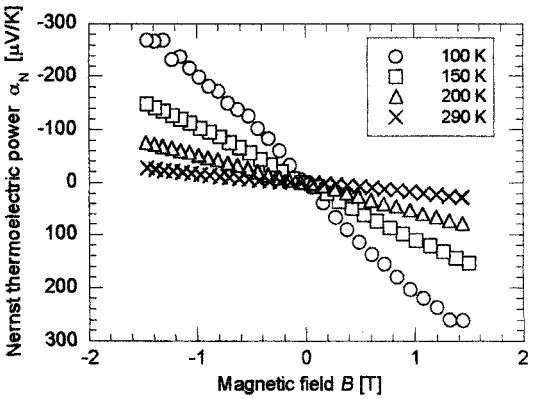

Fig. 4 Magnetic field dependences of the thermoelectric power of the Nernst effect α_N.

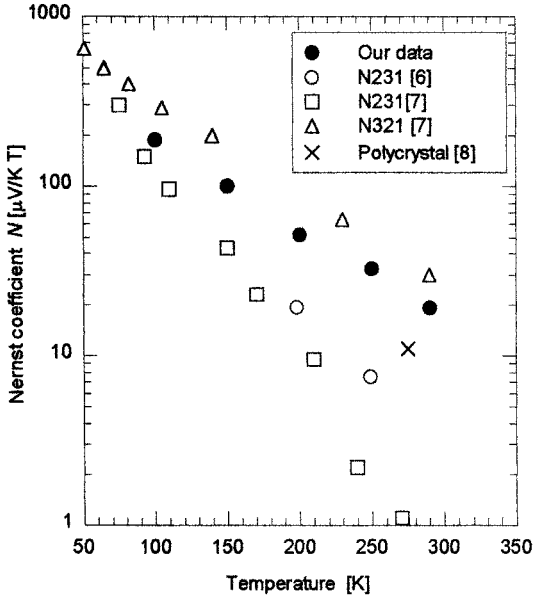

Fig. 5 Temperature dependence of the Nernst coefficient *N*. The other measurement values are also shown [6-8]. *N*231 and *N*321 correspond to *N* of the single crystal.

the trigonal direction and *N*321 corresponds when the heat flow in the bisectrix. The magnetic field is applied in the binary direction for both *N*231 and *N*321. The polycrystalline Bi has the high Nernst coefficient *N*, which is comparable to that of the single crystal Bi. At lower temperature, *N* rapidly increases. That means the Nernst element and the Nernst-Seebeck element using polycrystalline Bi are expected to be effective at low temperature

Figure 6 shows the magnetic field dependences of the diagonal resistance *R*. As the temperature decreases, *R* in the zero magnetic field decreases; whereas, the magneto-resistance remarkably increases for the lower temperature. In particular, the increase from the zero magnetic field reaches to 16 times for $B = \pm 1.5$ T at 100 K.

Figure 7 shows the magnetic field dependences of the thermal conductivity κ. Opposite to α_S or *R*, κ decreases in the magnetic field and tends toward the saturating for the zero magnetic field increases; whereas, the magnetic field effect increases for the lower temperature. We

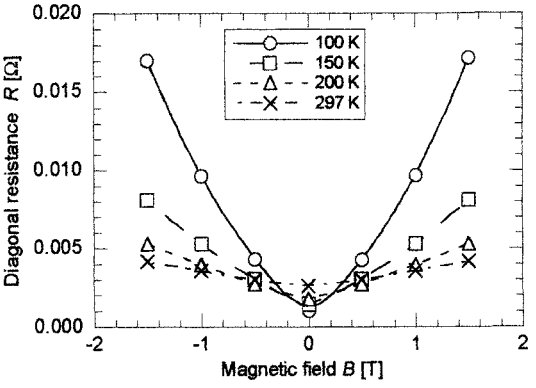

Fig. 6 Magnetic field dependences of the diagonal resistance *R*.

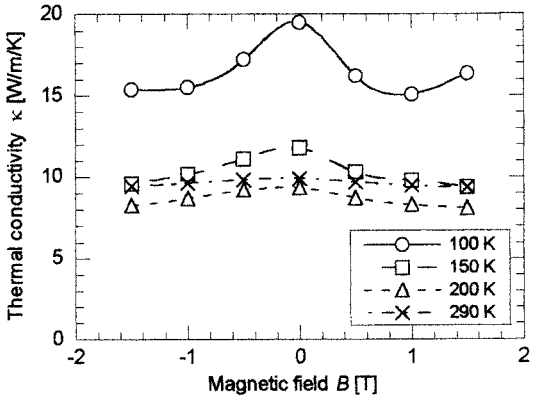

Fig. 7 Magnetic field dependences of the thermal conductivity κ.

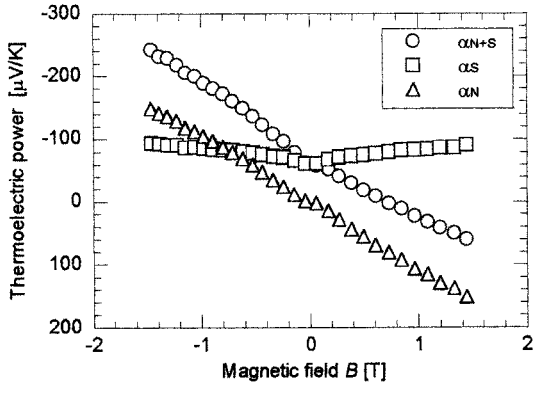

Fig. 8 Magnetic field dependences of the thermoelectric powers of the Seebeck effect α_S, the Nernst effect α_N, and the Nernst+Seebeck effect α_{S+N} at 150 K

compared the temperature dependence of κ, which we measured in the zero magnetic field, with the results by Brochin *et al.* for the polycrystal [4] and by Gallo *et al.* for the single crystal [13] to confirm the accuracy of our convenient measurement of κ. The temperature dependence of κ we measured is similar to that of the single crystal, while 50% higher than that of the polycrystal by Brochin *et al.*

4.2 Properties as the Nernst-Seebeck element

Figure 8 shows the magnetic field dependences of the thermoelectric powers of the Seebeck effect

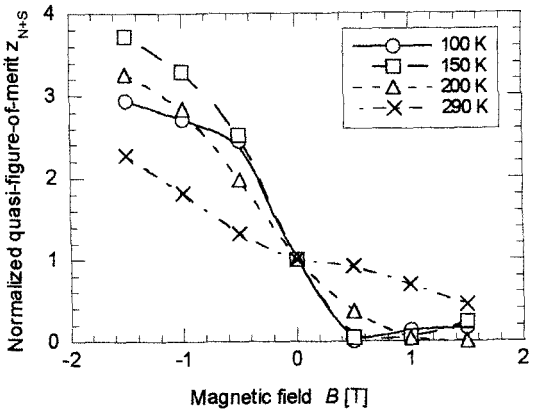

Fig. 9 Magnetic field dependences of the quasi figure-of-merit of the Nernst-Seebeck element z_{N+S}.

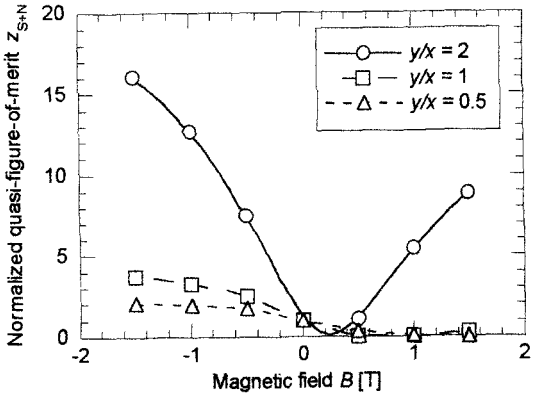

Fig. 10 The effect of the ratio of the geometry y/x in the magnetic field dependence of the measured quasi-figure -of-merit z_{N+S}.

(Seebeck coefficient) α_S, the Nernst effect α_N, and the Nernst+Seebeck effect α_{N+S} at 150 K. The thermo-electric power of the Nernst effect α_N exceeded α_S at ± 0.8 T and α_{N+S} for $B = -1.5$ T achieved 3 times of α_S in the zero magnetic field. Figure 9 shows the magnetic field dependences of the quasi-figure-of-merit of the Nernst-Seebeck element z_{N+S}. The quasi-figure-of-merit z_{N+S} in Fig. 9 is normalized by the value in the zero magnetic field to clarify the improvement by the magnetic field effect. Increase of z_{N+S} by the magnetic field is inclined to saturate at 100 K because of the remarkably large magnetoresistance. The maximum increase of z_{N+S} reached 3.7 times for $B = -1.5$ T at 150 K and z_{N+S} is expected to increase by applying the higher magnetic field at temperatures more than 150K.

4.3 Geometric effect of the Nernst-Seebeck element

The property of the Nernst-Seebeck element is expected to have a large geometry dependence on y/x from eq. (2), since NB of the polycrystalline Bi is found to be comparable for α_S at $y/x = 1$. Hence, variation of the geometry y/x is the next issue for the Nernst-Seebeck element. Besides of the sample with $y/x = 1$, which was examined above, we prepared another two samples with $y/x = 2$ (5 mm in length, 10 mm in width and 2 mm in thickness) and $y/x = 0.5$ (10 mm in length, 5 mm in width, and 2 mm in thickness). Figure 10 shows the effect of the ratio y/x in the magnetic field dependence of the measured quasi-figure-of-merit z_{N+S}. In the geometry $y/x = 2$, a remarkable increase of z_{N+S} was measured.

5. CONCLUSION

We proposed "the Nernst-Seebeck element", which aims to increase the effective thermoelectric power in the magnetic field by using the sum of the Nernst voltage and the Seebeck voltage. Transport coefficients and their magnetic field effects of a polycrystalline Bi were measured to estimate the performance of the Nernst-Seebeck element. As a result, 1) the Seebeck coefficient α_S increased, 2) the diagonal electric resistance R also increased, 3) the thermal conductivity decreased, and 4) the measured thermoelectric power of the Nernst effect NB was comparable to α_S. The quasi-figure-of-merit z_{N+S} were adopted to estimate the performance of the Nernst-Seebeck element instead of the thermoelectric figure-of-merit. Increase of z_{N+S} reached 3.7 times at maximum for $B = -1.5$ T at 150 K. A comparison of the sample with the different geometries proved that the remarkable increase can arise for the large ratio of the geometry y/x

ACKNOLEDGEMENT

The authors would like to thank Professor K. Nakamura and Mr. T. Yamaguchi of Chubu University for helpful suggestions and supports. The authors also thank the President A. Iiyoshi of Chubu University for continuous encouragement. This research is partly supported by the New Energy and Industrial Technology Development Organization (NEDO) fellowship program.

References

[1] W. C. Hall, "CRC Handbook of thermoelectrics", Ed. D. M. Rowe, CRC Press, Inc. (1995), pp503-513.
[2] R. Wolfe and G. E. Smith, *Appl. Phys. Lett.*, **1**, 5-7 (1962).
[3] W. M. Yim and A. Amith, *Solid State Electronics* **15**, 1141-1165 (1972).
[4] F. Brochin, B. Lenoir, X. Devaux, R. Martin-Lopez, and H. Scherrer, *J. Appl. Phys.*, **88**, 3269-3275 (2000).
[5] I. Ya. Korenblit, M. E. Kunsnetsov, and S. S. Shalyt, *Sov. Phys. JETP*, **29**, 4-10 (1969).
[6] J. P. Michenaud, E. Cheruvier, and J. P. Issi, *Solid State Commun.*, **9**, (1971), pp. 1433-1435.
[7] K. Sugihara, *J. Phys. Soc. Japan*, **27**, (1969), pp. 362-370.
[8] J. C. G. de Sande and J. M. Guerra, *Phys. Rev. B*, **45**, (1992), pp. 11469-11473.
[9] S. Yamaguchi, *J. Plasma and Fusion Research*, **78**, (2002), pp. 19-35. (in Japanese)
[10] S. Yamaguchi, et al., *Jpn. J. Appl. Phys.*, to be submitted.
[11] T. C. Harman and J. M. Honig, "Thermoelectric and Themomagnetic Effects and Applications", Chapter 6, McGraw-Hill (1967), pp273-310.
[12] *ibid.*, Chapter 7, pp311-370.
[13] C. F. Gallo, B. S. Chandrasekhar, and P. H. Sutter, J. Appl. Phys., 34, 144- 152(1963)

(Received October 13, 2003; Accepted January 16, 2004)